



Article

Study of Sludge Particles Formed during Coagulation of Synthetic and Municipal Wastewater for Increasing the Sludge Dewatering Efficiency

Lech Smoczynski ¹, Sławomir Kalinowski ¹, Igor Cretescu ^{2,*} , Michał Smoczynski ³ , Harsha Ratnaweera ⁴, Mihaela Trifescu ¹ and Marta Kosobucka ¹

¹ Faculty of Environmental Management and Agriculture, University of Warmia and Mazury in Olsztyn, 10719 Olsztyn, Poland; lechs@uwm.edu.pl (L.S.); kalinow@uwm.edu.pl (S.K.); trifescumihaela@gmail.com (M.T.); marta.kosobucka@uwm.edu.pl (M.K.)

² Faculty of Chemical Engineering and Environmental Protection, “Gheorghe Asachi” Technical University of Iasi, 700050 Iasi, Romania

³ Faculty of Food Sciences, University of Warmia and Mazury in Olsztyn, 10719 Olsztyn, Poland; michal.smoczynski@uwm.edu.pl

⁴ Faculty of Sciences and Technology, Norwegian University of Life Sciences, 0454 Ås, Norway; harsha.ratnaweera@nmbu.no

* Correspondence: icre1@yahoo.co.uk or icre@ch.tuiasi.ro; Tel.: +40-741-914-342

Received: 30 August 2018; Accepted: 15 October 2018; Published: 9 January 2019

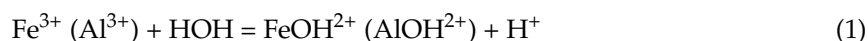


Abstract: Municipal wastewater sludge was produced by chemical coagulation of synthetic wastewater (*sww*) based on Synthene Scarlet P3GL disperse dye and real municipal wastewater (*nww*), coagulated by commercial coagulants PAX (prepolymerised aluminum coagulant) and PIX (a ferric coagulant based on $\text{Fe}_2(\text{SO}_4)_3$). An attempt was made to correlate the sludge's dewatering capacity (in terms of capillary suction time—CST) with operation parameters for wastewater treatment, size distribution and specific surface area of the sludge particles. It was found that the presence of phosphate ions in the system facilitates the removal efficiency of the above-mentioned dye (L) due to the interaction between the dye molecules and H_2PO_4^- ions. Unlike *sww*, negatively charged organic substances (*sorg*) in *nww* are directly adsorbed on the surface of colloidal particles $\{\text{Fe}(\text{OH})_3\}$ and $\{\text{Al}(\text{OH})_3\}$ (*prtc*). It was also discovered that an increase in the dose of a coagulant led to an increase of CST for *sww* sludge and to a decrease of CST for *nww* sludge. It has been suggested that flocs composed of spherical $\{\text{Al}(\text{OH})_3\}$ units possessed more internal space for water than aggregates consisting of rod-shaped $\{\text{Fe}(\text{OH})_3\}$ units and, consequently, it is more difficult to remove water from Al-*sww* sludge than from Fe-*sww*. The results obtained showed that smaller particles dominate in *sww* sludge, while larger particles are prevalent in *nww* sludge. To explain this distinct difference in the size distribution of particles in sludge obtained with the use of Al^{3+} and Fe^{3+} , simple models of aggregation and agglomeration-flocculation processes (*aaf*) of treated wastewater have been proposed. Except for PIX in *nww*, the analyzed particles of the investigated types of sludge were characterized by similar specific surface area (Sps), regardless of the kind of sludge or the applied coagulant. Slightly larger, negatively-charged *sorg* bridges, anchored directly on the surface of positive *prtc* are more effective in closing the structure of *nww* sludge than small L bridges of the dye molecules anchored on the surface of *prtc* via H_2PO_4^- . All the discovered aspects could lead to improved performance of wastewater treatment plants (WWTP) by increasing the efficiency of sludge dewatering.

Keywords: municipal wastewater sludge; dewatering; particle size distribution

1. Introduction

Chemical coagulation is the second step in wastewater treatment [1,2]. This process has a significant influence on the properties and structure of the resulting sludge [3–7]. The pH of sludge decreases during chemical coagulation because Fe^{3+} or Al^{3+} undergoes cationic hydrolysis and its first stage can be described as follows:



Positively-charged, colloidal particles $\{\text{Fe}(\text{OH})_3\}$ and/or $\{\text{Al}(\text{OH})_3\}$, described further as *prtc* (colloidal particles), are formed during the subsequent reactions which occur in wastewater [1,8]. These particles act as adsorbents [9] in the processes of aggregation and agglomeration-flocculation (*aaf*) of pollutants from wastewater. The surface charge of *prtc* is neutralized by negatively-charged components such as H_2PO_4^- , or by negatively-charged colloids, called *sorg* (organic substances). The removal of neutral or positively-charged pollutants takes place during the so-called flocculation [1,5,10]. This mechanism dominates also in the case of wastewater treatment by electrocoagulation [11–13], particularly during recirculating electrolysis of wastewater [14].

The quantity and quality of municipal wastewater sludge are indicators for the wastewater treatment performance and, on the other hand, determine the possibilities for further utilization of sludge [15]. For practical and technological reasons, the dewatering capability of sludge is extremely important [16]. This property of municipal wastewater sludge very much depends on the type and dose of inorganic coagulant added to the wastewater [17–19]. The structure of sludge flocs, as well as their physical and chemical characteristics, determine the efficiency of the dewatering process of municipal wastewater sludge [16,20]. Under laboratory conditions, so-called capillary suction time (CST) is a measure of the sludge's dewatering capacity [21]. Reproducibility and precision of CST measurements [22,23] are important, both for theoretical considerations [24] and in practice, e.g., for determination of an appropriate dose of an inorganic flocculant [25].

Probably the most important effect of flocs on the structure of municipal wastewater sludge is through aggregation and agglomeration-flocculation (*aaf*) processes [26–29]. Numerous papers have been published, including information about measurements, modeling and characterization of the structure of municipal wastewater sludge [30–33]. Often, the so-called fractal dimension D becomes a specific research instrument [34,35]. For self-similar objects, e.g., sludge floc-aggregates whose structure does not depend on a change in the scale, D is defined as follows:

$$M(R) \sim R^D \quad (2)$$

where M is the mass comprised in a sphere of the diameter R [34].

The value of D , either determined experimentally or calculated theoretically, has been used in many theoretical considerations, e.g., in kinetic calculations [36], and also in practical solutions, e.g., for the filtration of excessive active sludge [37]. The structure and properties of municipal wastewater sludge can also be examined directly through the determination of the distribution of the sizes of particles and their specific surface [38–40].

Since it is suspected that there is an interpretable correlation between the structure of municipal wastewater sludge and the value of CST corresponding to the sludge, this paper analyzes the observed correlations and proposes simple models of *aaf* processes for chemically-coagulated synthetic and real municipal wastewater.

The consecutive stages presented and considered in this article are based on:

- (a) results of traditional jar tests,
- (b) CST measurements,
- (c) determination of the volumetric dimension (D_v) and respectively of the specific surface area (S_p).

2. Materials and Methods

Synthetic dyeing wastewater (*sww*) and real municipal wastewater (*nww*) originating from a wastewater treatment plant in Reszel (North-Eastern Poland) were investigated. The municipal wastewater had the following parameters: suspended solids: SS (mg/L) = 250–800; total phosphorus: P (mg/L) = 9–13.5, chemical oxygen demand: COD (mgO₂/L) = 600–1800; turbidity: TU = 80–160 NTU; and pH = 6.6–7.8. In turn, each 1 L of *sww* contained 31.3 mg H₂PO₄[−] (10 mg P) and 50 mg disperse dye (L) (Synthene Scarlet P3GL) produced by the Boruta-Zachem Chemical Company, from Zgierz (Poland). Therefore, the composition of synthetic dyeing wastewater (31.3 mg H₂PO₄[−] + 50 mg disperse dye/L) is a result of the synergy effect of both components; a mixture of dye and municipal wastewaters is susceptible on coagulation and/or electrocoagulation, which has been proved and explained by previous studies [41]. It was experimentally demonstrated that in the absence of P-PO₄ it is impossible to remove even a small amount of dye L by chemical coagulation of its aqueous solution. However, coagulation of L solution proceeds effectively and efficiently in the presence of phosphate ions [42] and for this reason we decided to use this composition of synthetic wastewater in the present study.

The sludge samples submitted for further tests were obtained in wastewater coagulation by: (a) PIX 113, a ferric coagulant (based on Fe₂(SO₄)₃) widely used in Poland, and (b) PAX 18, pre-polymerised aluminum coagulant, an alternative to PIX. Both coagulants were produced by Kemipol, the Polish branch of the Kemira Chemicals in Gdansk, Poland. By adding the above-mentioned coagulants to the wastewaters, many intermediate polymeric species such as (Al(OH)₃)_n, (Fe(OH)₃)_m or (Fe(OH)₂)_p are produced, being responsible for colloidal sorption on their surfaces of pollutants from wastewaters.

In *sww*, the dye concentration was determined spectrophotometrically at a wavelength $\lambda = 460$ nm, while P-PO₄ was assayed according to the standard method ($\lambda = 690$ nm) using a HACH DR 3900 instrument (Hach Company, Loveland, CO, USA) with 13 mm standard cell tests.

After 30 min of sedimentation, followed by decantation, 25.0 cm³ of separated sludge was collected in order to determine capillary suction time CST [21–23], which is a measurement of the dewaterability of sludge. In CST measurements, a new prototype developed in the University of Warmia and Mazury in Olsztyn, Poland (DWTEST—Dewatering tester, schematically illustrated in Figure 1), was used.

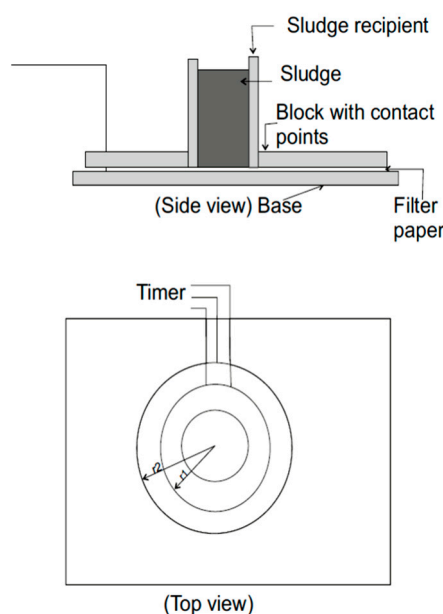


Figure 1. The schematic diagram of a new DWTEST prototype for measurement of the capillary suction time (CST).

In each case, 25 cm³ of separated sludge was applied onto a Whatman filter paper disc, while pressing the appropriate button on the apparatus. After several dozen seconds, the value of measured time corresponding to the flow of the liquid between electrodes in the measuring cell was displayed. The measurements were always repeated three times and the values for standard deviation (SD) (s) are indicated in the graphs. The results of CST measurements are presented in the graphical form in dependence of coagulant dose $CST = f(\text{mg Al or Fe/L})$.

Particle size distribution of the sludge was determined by measurement of laser light dispersion using a Mastersizer 3000 unit, Malvern Instruments, Malvern, United Kingdom [43]. Sludge samples were instilled to a measuring cell until an obscuration of 5–15% was achieved. The refractive indices for water and wastewater were 1.33 and 3.80, respectively. The particle size distribution was used to determine the mean particle size $D_{(3,2)}$ (μm) and available surface area (Sps) of particles in the sludge (m²/g). Mean particle size is defined as [43]:

$$D_{(3,2)} = n_i d_i^3 / \sum n_i d_i^2 \quad (3)$$

where n_i is the number of particles of diameter d_i .

Volumetric dimensions Dv_{10} , Dv_{50} and Dv_{90} denoting the maximum particle diameter below which particles account for 10%, 50% and 90% of the volume of the analyzed sludge, respectively, were also calculated. The results represent the mean values of three replications for each type of sludge evaluated.

3. Results and Discussion

The results of the laboratory tests are presented in Tables 1 and 2 and some of them in Figure 2. The mean values from three repetitions were used for plotting the graphs and SD values (in % or s) were marked in each case.

Figure 2 illustrates the effects of coagulation of *sww* and *nww* by coagulants PIX and PAX.

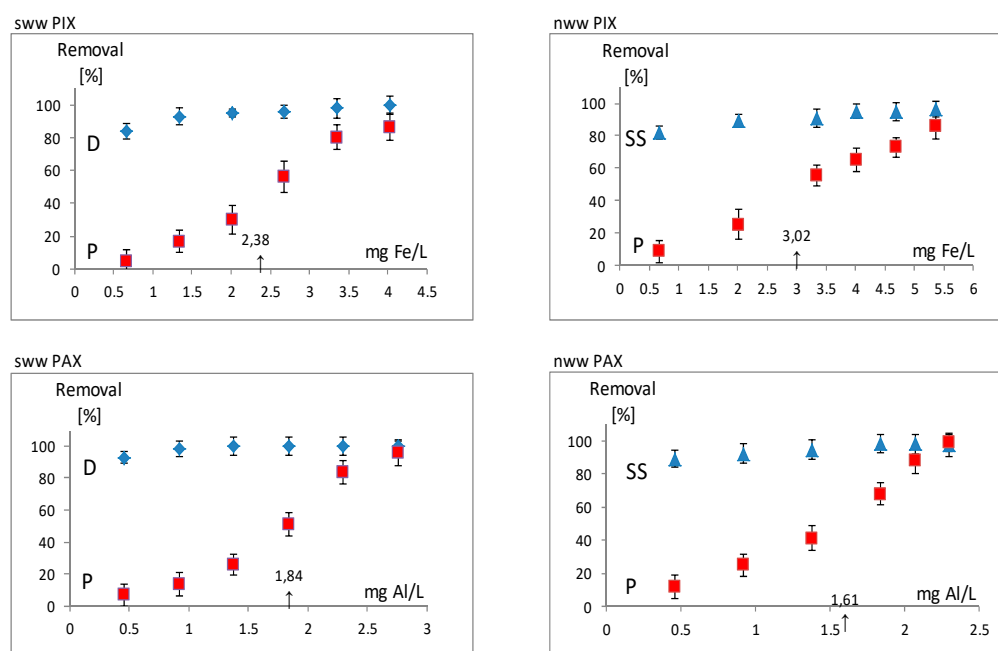


Figure 2. Synthetic wastewater (*sww*) and real municipal wastewater (*nww*) coagulated by PIX and PAX.

The initial (_o) and final (_f) values of the pH, concentration of total phosphorus (P), chemical oxygen demand (COD) and suspended solids (SS) are presented for both PIX and PAX coagulants used for treatment of both *sww* and *nww*:

$$\text{PIX-}sww: \text{pH}_o = 5.2 \rightarrow \text{pH}_f = 4.75 \quad \text{PAX-}sww: \text{pH}_o = 5.2 \rightarrow \text{pH}_f = 5.0$$

$$\text{PIX-}nww: \text{SS}_o = 750, \text{P}_o = 11.40; \text{COD}_o = 1690 \rightarrow \text{COD}_f = 360 \text{ (mgO}_2\text{/L);}$$

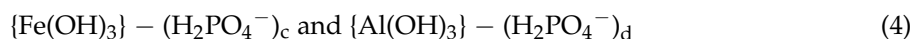
$$\text{pH}_o = 7.53 \rightarrow \text{pH}_f = 6.84$$

$$\text{PAX-}nww: \text{SS}_o = 440, \text{P}_o = 9.75; \text{COD}_o = 1190 \rightarrow \text{COD}_f = 313 \text{ (mgO}_2\text{/L);}$$

$$\text{pH}_o = 7.80 \rightarrow \text{pH}_f = 7.14$$

Courses of all four dependences, where Removal = f(coagulant dose), showed that the highest dose of both aluminum ions and ferric ions ensured 100% removal of L from *sww* and SS from *nww*. Under these conditions, PIX removed 86–87%, and PAX 96–99% of phosphorus (P) from both *sww* and *nww*. Because the limit of P allowed in the effluents according to Polish legislation for wastewater treatment plants (WTP) is 5 mg P/L, the sludge analyzed in our research was precipitated under conditions ensuring 50% removal of P from treated wastewater. It can be assumed that primary coagulation of municipal wastewater in Poland is sufficient to obtain the required P level in effluent, principally owing to the mentioned 50% coagulation of phosphorus compounds. In all of the four diagrams seen in Figure 2, an arrow on the x-axis indicates the numerical value of the dose of a coagulant (*fes*, *fen*, *als*, *aln*) adequate for attaining 50% of phosphorus removal from *sww* and *nww*. When these doses are added, i.e., to *sww*: *fes* = 2.38 mg Fe/L \equiv 0.0425 mmol Fe/L and *als* = 1.84 mg Al/L \equiv 0.068 mmol Al/L; and to *nww*: *fen* = 3.02 mg Fe/L \equiv 0.054 mmol Fe/L and *aln* = 1.61 mg Al/L \equiv 0.060 mmol Al/L, sediments were obtained, which were subsequently tested to determine CST, Sps and Dv (Table 1) as well as percentage shares of particular particle sizes.

During the coagulation process of *sww*, the presence of phosphate ions in the system made it possible to effectively remove the dye from the liquid phase of wastewater. Phosphate anions are adsorbed on positively-charged colloidal particles {Fe(OH)₃} and/or {Al(OH)₃} (*prtc*), creating units of the type:



As the negative sorbate (phosphate) accumulates on *prtc*, the positive potential of the systems in Formulas (4) decreases and mutual repulsive forces weaken between particles, which determine the direction, range and intensity of Brownian motions. Thus, the stability of the colloidal system decreases, while the probability of collisions between particles rises and finally an *aaf* process may occur.

In practice, an aqueous solution of phosphate ions undergoes coagulation (both precipitation and adsorption) and almost all phosphates could be transferred into municipal wastewater sludge.

As mentioned at the beginning of the Materials and Methods Section, in the absence of P-PO₄ it was impossible to remove even a small amount of a dye directly, by chemical coagulation of a water solution of L, whereas the coagulation or electro-coagulation of L [42] proceeded efficiently only when “supported” by phosphate ions. To explain the reasons for this phenomenon, the following simple model of adsorption of a dye particle to systems is proposed in Formulas (5) and (6):



This model assumes a slightly positive surface charge of a dye molecule, which repels it from a positive *prtc* while attracting it to *prtc* centers absorbing H₂PO₄[−]. It is thus based on the assumption that dye molecules can be adsorbed to units, Formulas (4), by forming bridges with the help of previously adsorbed H₂PO₄[−] ions (Formulas (5) and (6)). Although the occurrence of dye molecules, bridged on the surface of *prtc* with the help of H₂PO₄[−] slightly decreases the process of neutralization of the system’s surface, it also causes the growth of its mass and size, which is conducive to destabilization of *prtc* and leads to *aaf*. Thus, in laboratory practice, slightly more coagulant is used to achieve destabilization of a mixture of dye and H₂PO₄[−] than for a solution containing only H₂PO₄[−].

Figure 3a shows volumetric proportions for a spherical colloidal particle $\{\text{Al}(\text{OH})_3\}$ (sized from 86 to 206 μm , for which the diameter was assumed to be around 165 nm [44], which in fact, has a rather corrugated surface), a molecule of the dye (having an estimated 1 mole \approx 500 g and a size of about 10 nm) and a H_2PO_4^- ion (with a diameter of 1.2 nm). In the subsequent models presented in this paper (Figure 3b), for better clarity of the visualization, rod-shaped particles $\{\text{Fe}(\text{OH})_3\}$ [45] and spherical particles $\{\text{Al}(\text{OH})_3\}$ [44] are presented in appropriately diminished sizes, which is highlighted by using a broken line to draw their contours.

As expected, amounts of mg Fe/L from PIX (*fes* and *fen*) needed to remove 50% of P were higher than the respective amounts of mg Al/L from PAX (*als* and *aln*). Simultaneously, the same amounts expressed in mmol/L were higher for PAX than for PIX. In Poland PIX, rather than PAX, is a more popular coagulant in urban wastewater treatment plants (despite being less efficient) because of its much lower price per 1 kg of coagulant.

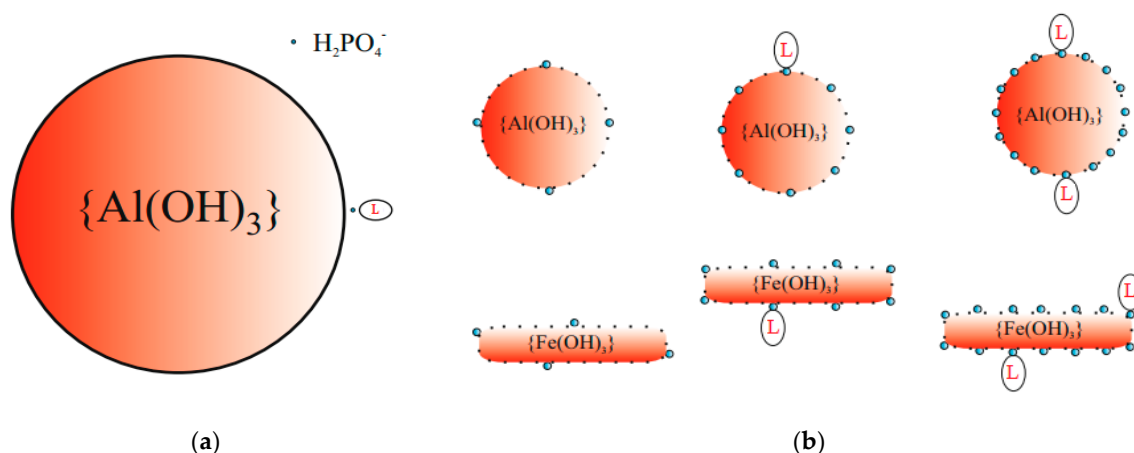


Figure 3. Schematic diagrams of interactions between colloidal particles and a dye molecule and H_2PO_4^- ion, respectively: (a) Approximate proportions between sizes of: colloidal particle $\{\text{Al}(\text{OH})_3\}$, dye L molecule and H_2PO_4^- ion; (b) schemes of structures for Formulas (4) and (5) responsible for adsorption of H_2PO_4^- and L from *sww* on the surface of colloidal particles (*prtc*).

Slightly more mg/L PIX was applied to remove 50% P from *nww* than from *sww*. Most probably, a part of the PIX dose in *nww* had been sacrificed to remove 1.330 mg/L *sorg* denoted as COD; $\text{COD}_0 = 1690 \rightarrow \text{COD}_f = 360 \text{ mgO}_2/\text{L}$ (Figure 2). Meanwhile, the same sample was characterized by a slightly higher concentration of phosphorus ($P_0 = 11.4 \rightarrow P_f = 0.64 \text{ mg/L}$) and SS_0 (750 mg/L) than the sample treated by PAX ($P_0 = 9.75 \rightarrow P_f = 0.22 \text{ mg/L}$, $\text{SS}_0 = 440 \text{ mg/L}$). For *nww* a slightly lower dose of PAX in mg/L, than from *sww*, was needed to remove 50% of phosphorus, which was most probably a consequence of lower consumption of the coagulant for removing just 887 mgO_2/L COD from *nww* ($\text{COD}_0 = 1190 \rightarrow \text{COD}_f = 313 \text{ mgO}_2/\text{L}$) at an approximately similar efficiency as PIX in the removal of L from *sww*.

Figure 4 contains a schematic representation of the removal of phosphorus as well as *sorg* from *nww* using PIX and PAX, respectively. Unlike L being bridged in *sww* by H_2PO_4^- , negatively charged *sorg* in *nww* are directly adsorbed on the surface of *prtc*. The schemas shown in Figure 4 also account for the hydrophilic properties of wastewater sol (*sorg*), marking in yellow the water molecules which stabilize this sol. Because of the negative charge of *sorg* here (*nww*), fewer H_2PO_4^- are adsorbed on the surface of *prtc* (only 7 H_2PO_4^- ions in the schema in Figure 4), compared to the respective surfaces of *prtc* formed during *sww* coagulation.

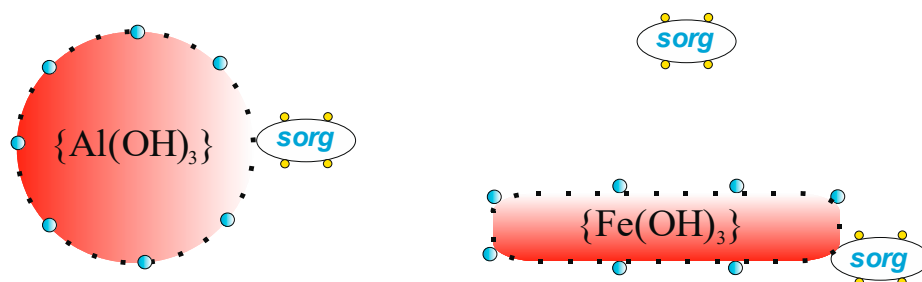


Figure 4. Schemas of structures responsible for adsorption of H_2PO_4^- and organic substances (*sorg*) from *nww* on the surface of *prtc*.

The following graphs in Figure 5 show the process of dewatering *sww* and *nww*, presented in the form of $\text{CST} = f(\text{dose of coagulant})$ relationships.

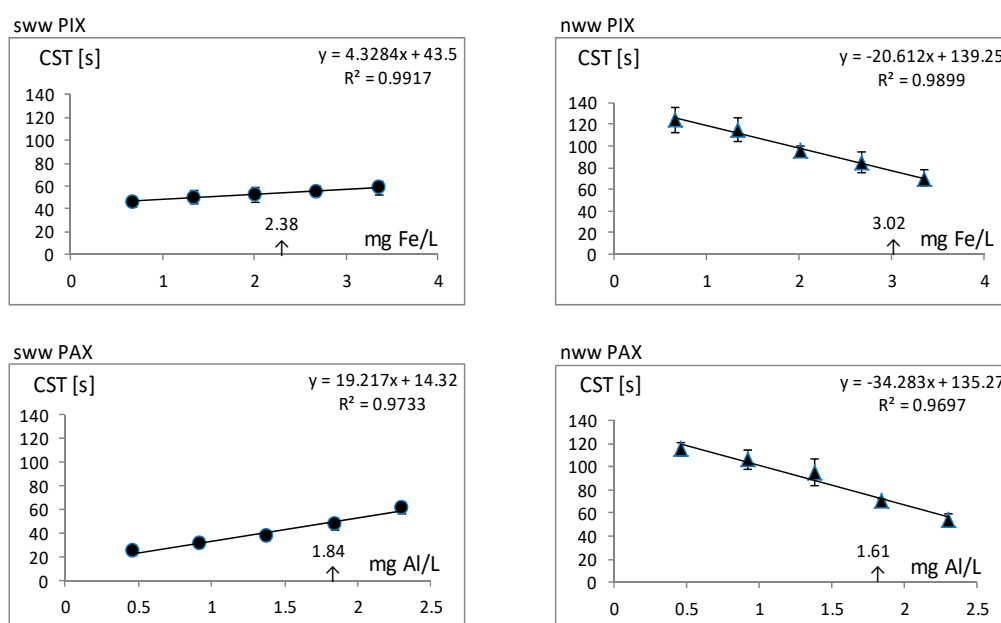


Figure 5. Dewatering of sludge obtained from *sww* and *nww* coagulated with PIX and PAX.

In both cases, the doses of coagulants (0.67 to 3.35 mg Fe/L and 0.46 to 2.3 mg Al/L) are within the range of doses used in the coagulation tests illustrated in Figure 2. According to Figure 5, the low values of SD (s), show a high repeatability of the measurements for capillary suction time CST, carried out by DWTEST instrument. For *sww* wastewater, the tendency of the relationship $\text{CST}_{sww} = f(\text{dose of coagulant})$ demonstrates a linear increase in CST, when the dose of coagulant is increased. Conversely, the increase in the dose of added coagulate to *nww* causes a linear decrease in CST_{nww} . The high values of the regression correlation coefficient R^2 , (which are ranged between 0.9697 and 0.9917), provide the linear character confirmation for the regression relationship $\text{CST} = f(\text{dose of coagulant})$. For *fes*, the CST_{sww} was 53.5 s, and for *als* it was 58 s.

With increasing doses of coagulant, CST_{sww} increased from 46 to 58 s for PIX and over a slightly wider range from 25 to 61 s for PAX. Undoubtedly, the structure of *sww* sludge obtained with PIX is different from the structure of sludge achieved with PAX, although the mechanism of bridging particular units is similar. As the dose of a coagulant increased, the share of these units in structures of sludge increased, which may have led to the blocking of water molecules in sludge flocs and a subsequent increase in CST. It is known that micelles $\{\text{Fe}(\text{OH})_3\}_n$ and $\{\text{Al}(\text{OH})_3\}_n$ differ from each other in shape and dimension [44,45]. The regression equations (Figure 5) allow the CST to be easily calculated for an identical dose of both coagulants, which is 0.05 mmol/L (within the range of *fes* = 0.045

and $als = 0.068$): $CST_{Fe} = 55.5$ s, and $CST_{Al} = 40.3$ s. The next calculation can be made for the same dose of both coagulants, equal to 0.1 mmol/L. Here, $CST_{Fe} = 67.7$ s, and $CST_{Al} = 66.2$ s, which almost the same. By extrapolating the CST values to higher coagulant doses, it can be hypothesized that *sww* sludge with PIX binds water more effectively at lower Fe doses, while *sww* sludge with PAX binds water more effectively at higher Al doses. Due to the small number of components in *sww* sludge as described in Formula (7):



the only explanation of the $CST = f(\text{dose of coagulant})$ is the structure of this sludge.

The structures illustrated in Figure 6 schematically describe the progressing *aaf* processes. It is clear that repulsion, as well as the intensity and scope of Brownian motions, decrease as the dose of a coagulant increases. The network of bridging and connections grows in the emerging aggregates-flocs of sediment *sww*. The schemas in Figure 6 may illustrate the destabilization of a single cluster (previously presented in Figure 3) due to the formation of appropriate dimers, in which a dye molecule most probably can bridge two *prtc* partly destabilized by H_2PO_4^- . At an increasing dose of a coagulant, these structures are most probably bridging, thus binding water in the internal spaces of agglomerate-flocs. It is known that rod-shaped colloidal particles, e.g., $\{\text{Fe}(\text{OH})_3\}$, coagulate more rapidly than spherical units $\{\text{Al}(\text{OH})_3\}$. However, the aggregation of many “rods” ultimately leads to the formation of a spherical aggregate-floc. Most probably, spherical aggregates composed of spherical units $\{\text{Al}(\text{OH})_3\}$ leave more internal space for water than other spherical aggregates composed of rod-shaped $\{\text{Fe}(\text{OH})_3\}$, which is why it is more difficult to remove water from Al-*sww* (longer CST) than from Fe-*sww* (shorter CST).

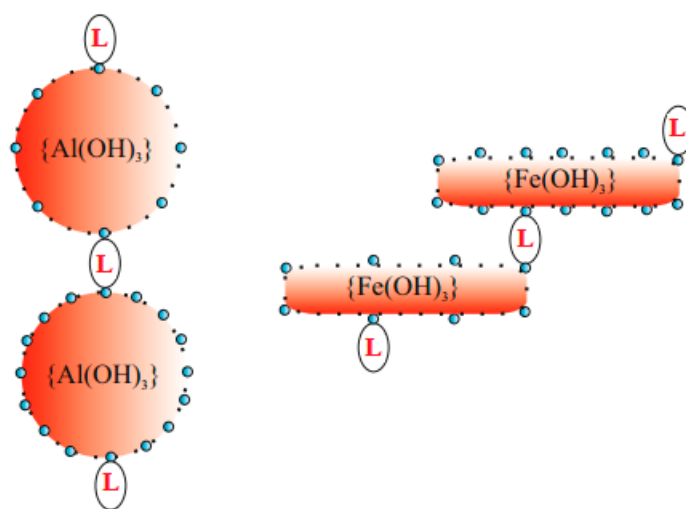


Figure 6. Schema of the progress of *aaf sww*.

As mentioned above, in contrast to *sww* sludge, an increase in the dose of a coagulant (both PIX and PAX) added to *nww* caused a linear decrease CST_{nww} . The CST_{sww} for *fen* was 77 s, and for *aln* it was 80 s. As the dose of a coagulant increased, the CST_{nww} decreased from 124 to 70 s for PIX, and from 115 to 54 s for PAX. In comparison with *sww*, in this case the variation of CST values for sludge obtained with PIX and PAX was distinctly smaller. From an appropriate regression equation (Figure 5), for identical doses of both coagulants (0.05 mmol/L), the following values of CST were calculated: $CST_{Fe} = 81.5$ s and $CST_{Al} = 89$ s. Analogously to *sww* tests, the subsequent calculations were made for the same dose of the coagulants equal to 0.1 mmol/L. The results were $CST_{Fe} = 23.8$ s and $CST_{Al} = 42.7$ s, which means that CST_{Al} is distinctly higher than CST_{Fe} . When extrapolating CST values to higher coagulant doses, it appears that at higher coagulant doses *nww* sludge with PAX may bind water more effectively than *nww* sludge with PIX. Compared to *sww*, *nww* sludge is a much more complex, multi-component system. From this point of view, the most significant

constituent of *nww* sludge is *sorg*. Most probably, the participation of *sorg* in the *aaf* process, leading to the formation of *nww* sludge, is responsible for the negative regression of the course of the $CST = f(\text{dose of coagulant})$ function.

Figure 7 shows a suggested schema of the *aaf* processes occurring during *nww* coagulation. Similarly to *sww*, an increase in the dose of a coagulant leads to a decrease in repulsion as well as the intensity and scope of Brownian motions in the system. The network of branches and connections in the *sww* sludge is expanding. The schema in Figure 7 may illustrate the destabilization of a single unit from Figure 4 through the formation of appropriate dimers, in which *sorg* most probably bridges two *prtc* partly destabilized by $H_2PO_4^-$. At an increasing dose of the coagulant, these structures most probably begin to branch, binding water in internal spaces within agglomerates-flocs. Organic compounds, *sorg*, which in total constitute so-called the “negative wastewater colloid” of *nww*, are classified as hydrophilic colloids, stabilized by the hydration shell of water molecules. As the negative wastewater colloid is progressively destabilized, and the *aaf* processes are in progress, the concentration of *sorg* decreases and water molecules released from the hydration shell become “available”, which leads to a decrease in CST. The increasing difference in the values of CST_{Fe} and CST_{Al} at increasing doses of a coagulant can be explained in this case as for *sww*. Gradually branching (Figure 7) structures containing spherical $\{Al(OH)_3\}$ units absorbing components of *nww* block the “inner-network” water more effectively than rod-shaped units with $\{Fe(OH)_3\}$.

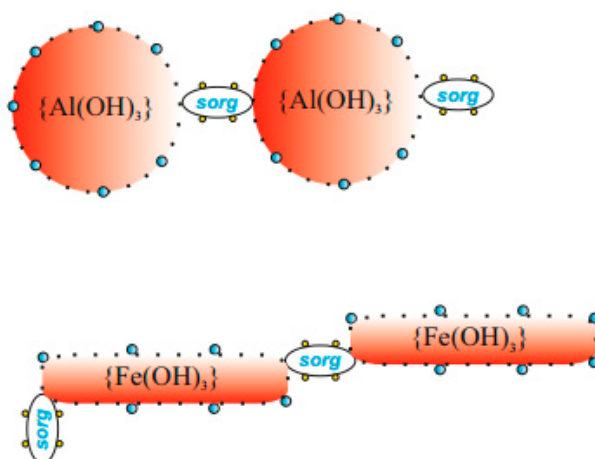


Figure 7. Schema of the progress of *aaf* processes in *nww*.

Figure 8 shows the percentages of specific size classes of particles in sludge obtained in the coagulation of *sww* and *nww*; using a) *fes* and *als*, and b) *fen* and *aln*. For both coagulants and in both types of wastewater, two classes of sludge particle size can be distinguished. The *sww* type of sludge is dominated by particles of a smaller size: 3–40 μm , but with a maximum of 3.72% at 12.7 μm for PIX, and 5–75 μm with a maximum of 6.38% at 24.1 μm for PAX. On the other hand, *nww* is dominated by sludge particles larger in size, in the range of 45–1300 μm for both coagulants. For the very low doses of a coagulant applied, the dominant size of *nww* sludge particles within the first range of sizes is difficult to define. For both coagulants, about 3.5% of sludge particles are sized about 130 μm , and are located within the second range.

Distributions of sludge particle size classes were very similar to the ones achieved for *nww* which were obtained in real municipal wastewater coagulated with the minimal doses of PIX (13.55 mg Fe/L) and PAX (2.45 mg Al/L), respectively [40]. It can be observed that these doses were much higher than the doses used in this study (3.02 mg Fe/L and 1.61 mg Al/L, respectively).

At the lower coagulant dose, larger size particles > 100 μm were prevalent as well. On the other hand, distributions of sludge particle classes similar to the ones identified in *sww* have also been recorded previously [39] in sludge obtained from synthetic wastewater coagulated with minimal doses

of PIX (6.5% of particles about 4 μm in size) and PAX (10% of particles about 10 μm in size). Certain similarities and differences in particle size classes between *sww* and *nww* sludge discussed here are most probably a consequence of very low doses of coagulant; in this study, a coagulant dose was high enough to remove only 50% of P. Development of this issue will be completed by using the values Sps and Dv, which are collected in Table 1.

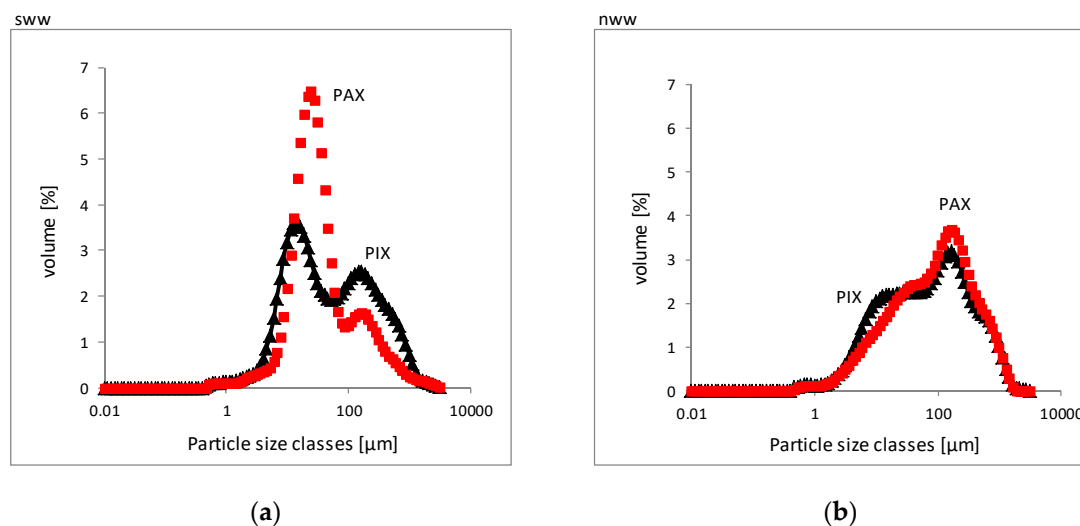


Figure 8. Sizes of flocs of sludge obtained from *sww* and *nww* coagulated with the help of: (a) *fes* and *als*, (b) *fen* and *aln*.

Table 1. The specific surface area (Sps) and volumetric dimension (Dv) values, for sludge particles illustrated in Figure 8.

Properties	PIX	PAX	PIX	PAX
	<i>sww</i> /SD	<i>sww</i> /SD	<i>nww</i> /SD	<i>nww</i> /SD
Sps ($\text{m}^2 \cdot \text{g}^{-1}$)	355/13.9	283/10.0	283/10.0	350/12.2
Dv10 (μm)	8.4/1.7	9.4/1.2	9.4/1.2	7.4/1.2
Dv50 (μm)	48.9/3.3	99.9/4.5	99.9/4.5	77.3/4.8
Dv90 (μm)	702/17.5	537/15.8	537/15.8	548/6.9

Table 1 presents Sps and Dv (including SD values) for particles of sludge obtained in the conditions illustrated in Figures 2 and 5 and specified in Figures 6 and 7.

The values of Sps (ranged between 283 and 355 m^2/g), were similar to the Sps values of 260–360 m^2/g , achieved for sludge obtained at coagulation of real municipal wastewater [40]. It is note worthy that such Sps values were obtained for all doses (i.e., minimal, optimal and maximal) of each coagulant PIX and PAX, respectively. Dv90 *sww* (Table 1), was slightly higher than Dv90 *nww*, which means that the applied doses of both coagulants formed slightly more uniform/homogenous particles in *nww* sludge than in *sww* sludge. It may also be suggested that the overall diversity of structures of the particles in *sww* sludge is higher than the diversity of particles in *nww* sludge.

Figure 9 contains a schematic presentation of the development of flocs in *sww* and *nww* sludge obtained with PIX. The low Dv90 value for *nww* indicated a generally higher uniformity of flocs in sludge built on *sorg* bridges than in sludge built on D bridges. The Dv90-based floc uniformity concept generally indicates the upper limit for the diameter and thus, within the specified range, limits the degree of raggedness or branching of these objects.

Since it is not an easy task to illustrate this problem, the objects presented in Figure 9 to a large extent are schematic representations. It seems likely that slightly larger, negatively charged *sorg* bridges, anchored directly on the surface of positive *prtc* more effectively close the sludge structures than the

smaller L bridges anchored on the *prtc* surface by the HPO_4^- , because L is rather unattractive for positive *prtc*.

Thus, the left part of Figure 9 shows the closed, and the right part shows the partly open, structure of two aggregates of *nww* sludge, similar in size, and an analogous, closed and completely open structure of two aggregates of *sww* sludge. For such structures, D_{v90} of *nww* would be lower than D_{v90} of *sww*, represented by the “open aggregate” in the lower, right-hand corner of Figure 9. At the same time, the higher D_{v90} value of *sww* sludge may generally indicate greater structural differentiation in *sww* sludge than in *nww* sludge.

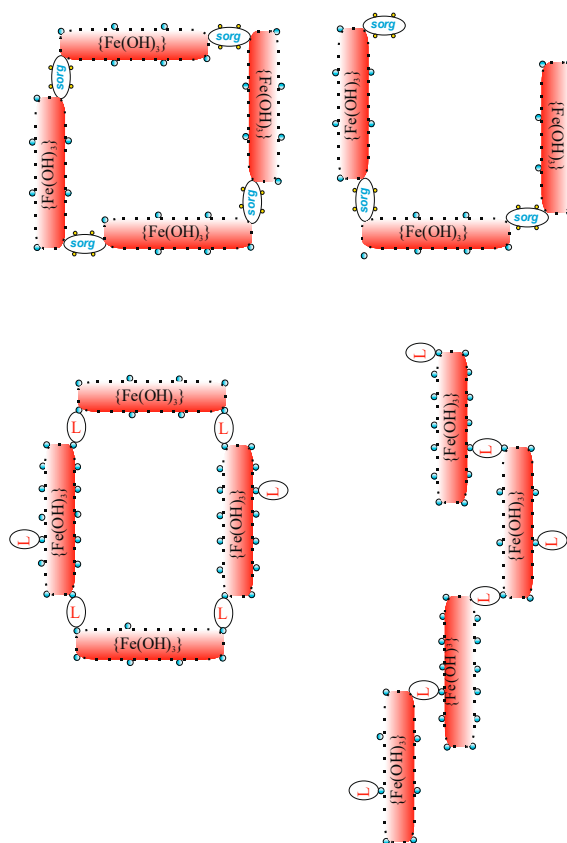


Figure 9. Schemas of more homogenous structures of *nww* sludge ($D_{v90} = 537 \mu\text{m}$) and less homogenous *sww* sludge ($D_{v90} = 702 \mu\text{m}$) obtained after coagulation with PIX.

Unquestionably, the progress of *aaf* processes is a direct consequence of the primary process forming the units illustrated in Figures 3 and 4. Due to a large deficit of the coagulant (an amount needed to remove just 50% of P), the conditions applied in this study can be referred to as “sub-stoichiometric”. In line with the Langmuir’s theory of adsorption, under such conditions we should expect complete saturation/use of the surface of *prtc* by adsorbed substances; i.e., L and P-PO_4 in *sww* flocs, and SS, *sorg* and P in *nww* flocs. In this case, individual units of flocs being formed should be characterized by higher porosity than units formed under “stoichiometric” conditions, especially in excessive amounts of a coagulant [37,39]. Porosity of floc-cluster units may influence the growth of Sps. At the same time, the larger filling of the centers on the adsorbent surface (*prtc*) should favor the *aaf* processes, as the forces of mutual repulsion decrease between the “saturated” surfaces of the units. As a result, the final porosity of these units only exerts a slight effect on the size, and on the final Sps value, for closed floc structures formed under sub-stoichiometric conditions.

It has been explained [43] that flocs of the analyzed sludge are formed from the units presented in Figure 9. Filling the space with the mass of a sludge floc can be defined with the fractal dimension, D_f , previously defined in Equation (2). There are more data available [19,29,46–48] on the fractal

dimension values of various types of flocs, including the values of D_f in sludge of municipal wastewater. Depending on the measurement method applied, the type of a coagulant and other parameters of the process, the values of D_f can be equal with the following values: 1.72 [19]; 1.68–1.74 [3]; 1.50–1.87 [4]; 1.69–1.96 [20]; 1.7–1.8 [46], 1.67–1.90 [47] and 1.8 [48]. Both fundamentally and practically, it may be interesting to compare the number of units, schematically illustrated in Figures 3 and 4, in a single floc of *sww* and *nww* sludge. Based on the aforementioned D_f values, the following assumptions were made for simple calculations of the number of units in such “statistical” floc: $D_f = 1.75$ and $R = Dv50$. For comparative purposes, it seems sufficient to choose $R = Dv50$, as it is implied by the definition of Dv , according to which this value can be the closest to the R diameter of a “statistical” floc. The values of the number of n units in a statistical municipal wastewater sludge floc, as comprised in Table 2, were calculated from the following equation:

$$n = [R/r]^{D_f} \quad (8)$$

where: $R = Dv50$ in μm , while $r = 0.17 \mu\text{m}$ and is an approximate sum of diameters of individual components in a *sww* unit:

$$\begin{aligned} & r(\text{H}_2\text{PO}_4^-) + r\{\text{Al}(\text{OH})_3\} + r(\text{H}_2\text{PO}_4^-) + r(\text{D}) \\ & = 0.0012 + 0.165 + 0.0012 + 0.010 = 0.1685 (\mu\text{m}) \end{aligned} \quad (9)$$

Earlier, an assumption was made that $r(\text{sorg})$ is slightly larger than $r(\text{D})$. Simultaneously, considering the fact that the r of a unit of *nww* sludge:

$$r\{\text{Al}(\text{OH})_3\} + r(\text{sorg}) \quad (10)$$

does not contain $r(\text{H}_2\text{PO}_4^-)$ and in view of the lack of other data for calculations, the value of r for *nww* was also adopted as being equal to $0.17 \mu\text{m}$, because the dominant component of r of a *nww* floc always has to be $r\{\text{Al}(\text{OH})_3\}$.

Table 2. Number of units in a statistical floc of the analyzed sludge.

Coagulant/Wastewater Type	Dv50 (μm)	Number of Units in a Floc
PIX/ <i>sww</i>	48.9	20,091
PAX/ <i>sww</i>	32.4	9776
PIX/ <i>nww</i>	99.9	70,138
PAX/ <i>nww</i>	77.3	44,774

The data contained in Table 2 are not absolute values and can be used only for comparative purposes. They indicate a much denser filling of the space by units-clusters in a bigger floc ($Dv50$) of *nww* sludge than that of a smaller floc ($Dv50$) in *sww* sludge. Within a certain range, these data confirm the general hypothesis of higher homogeneity of *nww* sludge, than of *sww* sludge (Figure 9).

The data allowed a comparison of the structures of two types of municipal wastewater sludge. In all presented case studies, the obtained sludge after chemical treatment of wastewater contained 3–5% dry solids, of which an average of 45% of the dry solids content was organic.

The results of such studies, when advanced and developed, can aid the improvement of practical wastewater treatment technologies. Simple procedures of simultaneous online measurements of $Dv10$, $Dv50$, $Dv90$ and Sps could be easily implemented at wastewater treatment plants. If a wastewater treatment plant is equipped with such an online measuring system, it will allow:

- (1) additional monitoring of the coagulation-flocculation process,
- (2) broader assessment of the “health”/quality of activated sludge,
- (3) better control and regulation of the process of municipal wastewater sludge dewatering.

4. Conclusions

Molecules of dye are adsorbed to *prtc* by bridging, with the help of H_2PO_4^- ions previously adsorbed to these surfaces. Unlike in *sww*, negatively charged *sorg* in *nww* are directly adsorbed on the surface of *prtc*.

As the dose of a coagulant increased, the CST_{sww} increased, while the CST_{nww} decreased. The *sww* sludge with PAX binds water more effectively at higher Al doses. Aggregates composed of spherical $\{\text{Al}(\text{OH})_3\}$ units leave more internal space for water than aggregates built from rod-shaped $\{\text{Fe}(\text{OH})_3\}$ units and, in consequence, a higher dose of PAX (Al) means that it is more difficult to remove water from Al-*sww* sludge (longer CST) than from Fe-*sww* (shorter CST).

Particles that are smaller in size dominate in *sww* sludge, while larger particles prevail in *nww* sludge. Except for PIX in *nww*, the analyzed particles of the types of sludge tested were characterized by similar Sps, irrespective of the type of wastewater or the applied coagulant. Values of Dv_{90} for *sww* are slightly higher than Dv_{90} *nww*, which means that the differentiation of structures of *sww* sludge particles is greater than in *nww* sludge. Slightly larger, negatively charged *sorg* bridges, directly anchored on the surface of positive *prtc*, more effectively close structures of *nww* sludge than smaller L bridges, anchored on the surface of *prtc* via HPO_4^- ions. The porosity of units has only a slight influence on the size and final value of Sps of closed structures of flocs formed under sub-stoichiometric conditions. The larger statistical floc of *nww* sludge is more densely packed with units-clusters than the space of a smaller *sww* floc.

Author Contributions: This article was written by L.S. and H.R. based on the investigations carried out in the frame of Polish-Norwegian Research Program operated by the National Centre for Research and Development under the Norwegian Financial Mechanism 2009–2014. These authors designed the research project and conducted the laboratory tests and analyses developed by Ph.D students M.K. and M.T. S.K. designed the equipment and provided technical knowledge to support the experimental work. M.S. carried out optical investigations and visualization and I.C. participated in reviewing and final writing of this manuscript.

Funding: This research was mainly funded by Polish-Norwegian Research Program, grant number, POL-NOR/196364/7/2013.; 561755-1-2015-1-NO-EPPKA2-CBHE-JP, (2015-3386/001-001); and statutory grant 20610.001-300.

Acknowledgments: This work was supported by a Polish-Norwegian Research Program operated by the National Centre for Research and Development under the Norwegian Financial Mechanism 2009–2014 in the framework of Project Contract No. POL-NOR/196364/7/2013; “Harmonizing water related graduate education” under grant 561755-1-2015-1-NO-EPPKA2-CBHE-JP (2015-3386/001-001); and under statutory grant 20610.001-300.

Conflicts of Interest: The authors declare no conflicts of interest.

Nomenclature

<i>sww</i>	synthetic wastewater
<i>nww</i>	real municipal wastewater (natural origin)
CST	capillary suction time (s)
<i>aaf</i>	aggregation-agglomeration-flocculation
SD	standard deviation of the sample (% or mg/L)
<i>fes</i>	number of mg Fe^{3+} (PIX) which remove 50% P from 1 L of <i>sww</i>
<i>als</i>	umber of mg Al^{3+} (PAX) which remove 50% P from 1 L of <i>sww</i>
<i>fen</i>	number of mg Fe^{3+} (PIX) which remove 50% P from 1 L of <i>nww</i>
<i>aln</i>	number of mg Fe^{3+} (PIX) which remove 50% P from 1 L of <i>nww</i>
Dv	volumetric dimension (μm)
Sps	specific surface area (m^2/g)
L	disperse dye (Synthene Scarlet P3GL)
SS	Suspended Solids (mg/L)
<i>prtc</i>	colloidal particle $\{\text{Fe}(\text{OH})_3\}$ or $\{\text{Al}(\text{OH})_3\}$
<i>sorg</i>	organic substances (responsible for COD in <i>nww</i>)

References

1. Duan, J.; Gregory, J. Coagulation by hydrolyzing metal salts. *Adv Colloid Interface Sci.* **2003**, *100–102*, 475–502. [[CrossRef](#)]
2. The, C.Y.; Budiman, P.M.; Shak, K.P.; Wu, T.Y. Recent advancement of coagulation-flocculation and its application in wastewater treatment. *Ind. Eng. Chem. Res.* **2016**, *55*, 4363–4389.
3. Zheng, H.; Shu, G.; Jiang, S.; Tshukudu, T.; Xiang, X.; Zhang, P.; He, Q. Investigations of coagulation-flocculation process by performance optimization, model prediction and fractal structure of flocs. *Desalination* **2011**, *269*, 148–156. [[CrossRef](#)]
4. Chu, C.P.; Lee, D.J. Effect of pre-hydrolysis on floc structure. *J. Environ. Manag.* **2004**, *71*, 285–292. [[CrossRef](#)]
5. Zhao, Y.X.; Shon, H.K.; Wang, Y.; Kim, J.H.; Yue, Q.Y. The effect of second coagulant dose on the regrowth of flocs formed by charge neutralization and sweep coagulation using titanium tetrachloride (TiCl₄). *J. Hazard Mater.* **2011**, *198*, 70–77. [[CrossRef](#)]
6. Fytili, D.; Zabaniotou, A. Utilization of sewage sludge in EU application of old and new methods—A review. *Renew. Sustain. Energy Rev.* **2008**, *12*, 116–140. [[CrossRef](#)]
7. Verna, S.; Prased, B.; Mishra, I.M. Pretreatment of petrochemical wastewater by coagulation and the sludge characteristics. *J. Hazard Mater.* **2010**, *178*, 1055–1064. [[CrossRef](#)]
8. Rohrsetzer, S.; Paszli, I.; Csempeš, F.; Ban, S. Colloidal stability of electrostatically stabilized sol particles. Part I: The role of hydration in coagulation and reeptization of ferric hydroxide sol. *Colloid Polym. Sci.* **1992**, *270*, 1243–1251. [[CrossRef](#)]
9. Smoczyński, L.; Ratnaweera, H.; Kosobucka, M.; Kvaal, K.; Smoczyński, M. Image Analysis of Sludge Aggregates Obtained at Preliminary Treatment of Sewage. *Water Sci. Technol.* **2014**, *70*, 1048–1055. [[CrossRef](#)]
10. Amirtharajah, A.; Mills, M.K. Rapid-mix design for mechanism of alum coagulation. *JAWWA* **1982**, *74*, 210–216. [[CrossRef](#)]
11. Butler, E.; Hung, Y.T.; Yu, L.R.; Al Ahmad, M. Electrocoagulation in wastewater treatment. *Water* **2011**, *3*, 395–525. [[CrossRef](#)]
12. Zaleschi, L.; Teodosiu, C.; Cretescu, I.; Rodrigo, M.A. A Comparative Study of Electrocoagulation and Chemical Coagulation Processes Applied for Wastewater Treatment. *Environ. Eng. Manag. J.* **2012**, *11*, 1517–1525.
13. Smoczynski, L.; Munska, K.; Pierozynski, B. Electrocoagulation of synthetic dairy wastewater. *Water Sci. Technol.* **2013**, *67*, 404–409. [[CrossRef](#)]
14. Groterud, O.; Smoczyński, L. Removal of phosphorus and residual aluminium by a recirculating electrolysis of wastewater. *Vatten* **1986**, *42*, 293–296.
15. Mikkelsen, L.H.; Keiding, K. Physico-chemical characteristics of full scale sewage sludge with implications to dewatering. *Water Res.* **2002**, *36*, 2451–2462. [[CrossRef](#)]
16. Jin, B.; Wilen, B.M.; Lant, P. Impact of morphological, physical and chemical properties of sludge flocs on dewaterability of activated sludge. *Chem. Eng. J.* **2004**, *98*, 115–126. [[CrossRef](#)]
17. Turchiuli, C.; Fargues, C. Influence of structural properties of alum and ferric flocs on sludge dewaterability. *Chem. Eng. J.* **2004**, *103*, 123–131. [[CrossRef](#)]
18. Niu, M.; Zhang, W.; Wang, D.; Chen, Y.; Chen, R. Correlation of physiochemical properties and sludge dewaterability under chemical conditioning using inorganic coagulants. *Bioresour. Technol.* **2013**, *144*, 337–343. [[CrossRef](#)]
19. Zhao, Y.Q. Correlations between floc physical properties and optimum polymer dosage in alum sludge conditioning and dewatering. *Chem. Eng. J.* **2003**, *92*, 227–235. [[CrossRef](#)]
20. Zhao, P.; Ge, S.; Chen, Z.; Li, X. Study on pore characteristics of flocs and sludge dewaterability based on fractal methods (pore characteristics of flocs and sludge dewatering). *Appl. Therm. Eng.* **2013**, *58*, 217–223. [[CrossRef](#)]
21. Sawalha, O.; Scholz, M. Assessment of capillary suction time (CST) test methodology. *Environ. Technol.* **2007**, *28*, 1377–1386. [[CrossRef](#)]
22. Sawalha, O.; Scholz, M. Innovative enhancement of the design and precision of the capillary suction time testing device. *Water Environ. Res.* **2009**, *81*, 2344–2352. [[CrossRef](#)]
23. Scholtz, M.; Tapp, J. Development of the revised Capillary Suction Time (CST) test. *Water Cond. Purif.* **2006**, *48*, 46–52.

24. Tuan, P.-A.; Sillanpaa, M. Migration of ions and organic matter during electro-dewatering of anaerobic sludge. *J. Hazard Mater.* **2010**, *173*, 54–61. [[CrossRef](#)]
25. Lee, C.H.; Liu, J.C. Sludge dewaterability and floc structure in dual polymer conditioning. *Adv. Environ. Res.* **2001**, *5*, 129–136. [[CrossRef](#)]
26. Meakin, P. The effects of reorganization processes on two dimensional cluster—Cluster aggregation. *J. Colloid Interface Sci.* **1986**, *112*, 187–194. [[CrossRef](#)]
27. Yu, W.; Liu, T.; Gregory, J.; Li, G.; Liu, H.; Qua, J. Aggregation of nano-sized alum–humic primary particles. *Sep. Purif. Technol.* **2012**, *99*, 44–49. [[CrossRef](#)]
28. Pastor-Satorras, R.; Rubí, J.M. Particle-cluster aggregation with dipolar interactions. *Phys. Rev. E* **1995**, *51*, 5994–6003. [[CrossRef](#)]
29. Smoczyński, L.; Bukowski, Z.; Wardzyńska, R.; Załęska-Chróst, K. Dłużyńska, B. Simulation of coagulation, flocculation and sedimentation. *Water Environ. Res.* **2009**, *81*, 348–356. [[CrossRef](#)]
30. Jullien, R.; Meakin, P. Simple models for the restructuring of 3-dimensional ballistic aggregates. *J. Colloid Interface Sci.* **1989**, *127*, 265–272. [[CrossRef](#)]
31. Jarvis, P.; Jefferson, B.; Parsons, S.A. Measuring floc structural characteristics. *Rev. Environ. Sci. Bio-Technol.* **2005**, *4*, 1–18. [[CrossRef](#)]
32. Chu, C.P.; Lee, D.J. Structural analysis of sludge flocs. *Adv. Powder Technol.* **2004**, *15*, 515–532. [[CrossRef](#)]
33. Zhao, Y.Q. Settling behaviour of polymer flocculated water treatment sludge II: Effects of floc structure and floc packing. *Sep. Purif. Technol.* **2004**, *35*, 175–183. [[CrossRef](#)]
34. Mandelbrot, B.B. *The Fractal Geometry of Nature*; Freeman: San Francisco, CA, USA, 1982.
35. Leman, J.; Smoczynski, M.; Dolgan, T.; Dziuba, Z. Fractal analysis of structure of cow and goat β -lactoglobulin preparation. *J. Food Technol.* **2005**, *42*, 428–430.
36. Yang, Z.; Yang, H.; Jiang, Z.; Huang, X.; Li, H.; Li, A.; Cheng, R. A new method for calculation of flocculation kinetics combining Smoluchowski model with fractal theory. *Colloids Surf. A* **2013**, *423*, 11–19. [[CrossRef](#)]
37. Meng, F.G.; Zhang, H.M.; Li, Y.S.; Zhang, X.W.; Yang, F.L.; Xiao, J.N. Cake layer morphology in microfiltration of activated sludge wastewater based on fractal analysis. *Sep. Purif. Technol.* **2005**, *44*, 250–257. [[CrossRef](#)]
38. Smoczynski, L.; Ratnaweera, H.; Kosobucka, M.; Smoczynski, M.; Pieczulis-Smoczynska, K.; Cretescu, I. The size of aggregates formed during coagulation and electrocoagulation of synthetic wastewater. *J. Environ. Prot. Ecol.* **2016**, *17*, 1160–1170.
39. Wang, Y.; Gao, B.Y.; Xu, X.M.; Xu, G.Y. Characterization of floc size, strength and structure in various aluminum coagulants treatment. *J. Colloid Interface Sci.* **2009**, *332*, 354–359. [[CrossRef](#)]
40. Smoczynski, L.; Kosobucka, M.; Smoczynski, M.; Ratnaweera, H.; Pieczulis-Smoczynska, K. Sizes of particles formed during municipal wastewater treatment. *Water Sci. Technol.* **2017**, *75*, 971–977.
41. Smoczyński, L.; Ratnaweera, H.; Kosobucka, M.; Smoczyński, M.; Kalinowski, S.; Kvaal, K. Modelling the structure of sludge aggregates. *Environ. Technol.* **2016**, *37*, 1122–1132. [[CrossRef](#)]
42. Smoczyński, L.; Ratnaweera, H.; Kosobucka, M.; Smoczyński, M. Image analysis of sludge aggregates. *Sep. Purif. Technol.* **2014**, *122*, 412–420. [[CrossRef](#)]
43. Malvern Instruments Limited. *A Basic Guide to Particle Characterization*; Malvern Instruments Limited: Worcestershire, UK, 2012; pp. 1–26.
44. Macedo, M.L.F.; Osawa, C.C.; Bertran, C.A. Sol-gel synthesis of transparent alumina gel and pure gamma alumina by urea hydrolysis of aluminum nitrate. *J. Sol.-Gel. Sci. Technol.* **2004**, *30*, 135–140. [[CrossRef](#)]
45. Haas, W.; Zrinyi, M.; Kilian, H.G.; Heise, B. Structural analysis of anisometric colloidal iron(III)-hydroxide particles and particle-aggregates incorporated in poly(vinyl-acetate) networks. *Colloid Polym. Sci.* **1993**, *271*, 1024–1034. [[CrossRef](#)]
46. Waite, T.D. Measurement and implications of flock structure in water and wastewater treatment. *Colloids Surf. A* **1999**, *151*, 27–41. [[CrossRef](#)]
47. Smoczynski, L.; Wardzynska, R. Study on macroscopic aggregation of silica suspensions and sewage. *J. Colloid Interface Sci.* **1996**, *183*, 309–314. [[CrossRef](#)]
48. Gregory, J. The role of floc density in solid-liquid separation. *Filtr. Sep.* **1998**, *35*, 367–371. [[CrossRef](#)]

